

University of Nebraska - Lincoln

DigitalCommons@University of Nebraska - Lincoln

Christian Binek Publications

Research Papers in Physics and Astronomy

5-21-2019

Space-charge limited conduction in epitaxial chromia films grown on elemental and oxide-based metallic substrates

C.-P. Kwan
SUNY University at Buffalo

Mike Street
University of Nebraska - Lincoln

Ather Mahmood
University of Nebraska-Lincoln, ather.mahmood@unl.edu

Will Echtenkamp
University of Nebraska-Lincoln

M. Randle
SUNY University at Buffalo

See next page for additional authors

Follow this and additional works at: <https://digitalcommons.unl.edu/physicsbinek>

 Part of the [Condensed Matter Physics Commons](#)

Kwan, C.-P.; Street, Mike; Mahmood, Ather; Echtenkamp, Will; Randle, M.; He, K.; Nathawat, J.; Arabchigavkani, N.; Barut, B.; Yin, S.; Dixit, R.; Singiseti, Uttam; Binek, Christian; and Bird, J. P., "Space-charge limited conduction in epitaxial chromia films grown on elemental and oxide-based metallic substrates" (2019). *Christian Binek Publications*. 89.
<https://digitalcommons.unl.edu/physicsbinek/89>

This Article is brought to you for free and open access by the Research Papers in Physics and Astronomy at DigitalCommons@University of Nebraska - Lincoln. It has been accepted for inclusion in Christian Binek Publications by an authorized administrator of DigitalCommons@University of Nebraska - Lincoln.




Authors

C.-P. Kwan, Mike Street, Ather Mahmood, Will Echtenkamp, M. Randle, K. He, J. Nathawat, N. Arabchigavkani, B. Barut, S. Yin, R. Dixit, Uttam Singiseti, Christian Binek, and J. P. Bird

Space-charge limited conduction in epitaxial chromia films grown on elemental and oxide-based metallic substrates

Cite as: AIP Advances 9, 055018 (2019); <https://doi.org/10.1063/1.5087832>

Submitted: 04 January 2019 . Accepted: 09 May 2019 . Published Online: 21 May 2019

C.-P. Kwan, M. Street , A. Mahmood, W. Echtenkamp, M. Randle, K. He, J. Nathawat, N. Arabchigavkani, B. Barut, S. Yin, R. Dixit, U. Singiseti , Ch. Binek, and J. P. Bird 



View Online



Export Citation



CrossMark

ARTICLES YOU MAY BE INTERESTED IN

[Energy condition of isothermal magnetoelectric switching of perpendicular exchange bias in Pt/Co/Au/Cr₂O₃/Pt stacked film](#)

Journal of Applied Physics **124**, 233902 (2018); <https://doi.org/10.1063/1.5047563>

[A novel fluid structure interaction model for the grooved piston-cylinder interface in axial piston pump](#)

AIP Advances **9**, 055013 (2019); <https://doi.org/10.1063/1.5090596>

[Identifying short- and long-time modes of the mean-square displacement: An improved nonlinear fitting approach](#)

AIP Advances **9**, 055112 (2019); <https://doi.org/10.1063/1.5098051>

AVS Quantum Science

Co-published with AIP Publishing



Coming Soon!

Space-charge limited conduction in epitaxial chromia films grown on elemental and oxide-based metallic substrates

Cite as: AIP Advances 9, 055018 (2019); doi: 10.1063/1.5087832

Submitted: 4 January 2019 • Accepted: 9 May 2019 •

Published Online: 21 May 2019





View Online



Export Citation



CrossMark

C.-P. Kwan,¹ M. Street,²  A. Mahmood,² W. Echtenkamp,² M. Randle,³ K. He,³ J. Nathawat,³ N. Arabchigavkani,¹ B. Barut,¹ S. Yin,³ R. Dixit,³ U. Singiseti,³  Ch. Binek,² and J. P. Bird^{3,a)} 

AFFILIATIONS

¹Department of Physics, University at Buffalo, The State University of New York, Buffalo, New York 14260-1500, USA

²Department of Physics and Astronomy, Theodore Jorgensen Hall, 855 North 16th St., University of Nebraska-Lincoln, Lincoln, Nebraska 68588-0299, USA

³Department of Electrical Engineering, University at Buffalo, The State University of New York, Buffalo, New York 14260-1900, USA

^{a)}E-mail: jbird@buffalo.edu

ABSTRACT

We study temperature dependent (200 – 400 K) dielectric current leakage in high-quality, epitaxial chromia films, synthesized on various conductive substrates (Pd, Pt and V₂O₃). We find that trap-assisted space-charge limited conduction is the dominant source of electrical leakage in the films, and that the density and distribution of charge traps within them is strongly dependent upon the choice of the underlying substrate. Pd-based chromia is found to exhibit leakage consistent with the presence of deep, discrete traps, a characteristic that is related to the known properties of twinning defects in the material. The Pt- and V₂O₃-based films, in contrast, show behavior typical of insulators with shallow, exponentially-distributed traps. The highest resistivity is obtained for chromia fabricated on V₂O₃ substrates, consistent with a lower total trap density in these films. Our studies suggest that chromia thin films formed on V₂O₃ substrates are a promising candidate for next-generation spintronics.

© 2019 Author(s). All article content, except where otherwise noted, is licensed under a Creative Commons Attribution (CC BY) license (<http://creativecommons.org/licenses/by/4.0/>). <https://doi.org/10.1063/1.5087832>

I. INTRODUCTION

The magnetoelectric (ME)¹ chromia (Cr₂O₃)² is an antiferromagnetic oxide, whose bulk order parameter may be manipulated by the application of an electric field. At the same time, this dielectric is known to exhibit a robust boundary magnetization (at its (0001) crystalline surface), the direction of which may be controlled by the application of a suitable electric field.^{3–5} Recently, this boundary magnetization has been exploited to implement an all electrical scheme for the exchange biasing of a nearby magnetic multilayer,⁶ a result that represents a critical step for attempts to develop electrical control of magnetism for spintronics. This approach of voltage control of magnetism (VCM) has the potential to replace existing approaches to spintronics (such as spin transfer torque), which typically rely on the use of energetically-costly electrical currents for

magnetic switching. In contrast, the use of even large electric fields to switch the boundary magnetization of chromia should (ideally) arise without any associated current, allowing VCM to be achieved at low power levels (the reader is referred to Ref. 7 for a recent benchmarking of chromia-based spintronics.)

Chromia is a linear ME that exhibits a transition from the paramagnetic to the antiferromagnetic phase at a Néel temperature of $T_N = 307$ K,^{2,8} making it one of the few materials to exhibit magnetoelectricity at room temperature. Its boundary magnetization onsets with the appearance of the antiferromagnetic order, and is found to be insensitive to the presence of roughness.³ Dependent upon the oxygen partial pressure utilized during the growth process, and on the impurities present within the material, chromia can be either a *p*-type or an *n*-type semiconductor.^{9,10} In bulk form, at least, its large bandgap of ~ 3 eV¹¹ results in high intrinsic resistivity ($\rho \sim 10^{14}$ Ω cm

at 300 K),¹² a key requirement for the implementation of low-power schemes for VCM. For practical devices, however, it is necessary to realize chromia in thin-film form, and a key challenge here is to meet this objective while maintaining the dielectric character of the material. Previously, thin-film growth has been implemented by a number of methods,^{10,13–21} with significant variations being reported in the resistivity of the resulting films. Published values vary from $10^2 - 10^9 \Omega\text{cm}$, with resistivities at the lower end of this range being obtained by sputter deposition,¹⁴ while those at the upper end are synthesized via pulsed-laser deposition.¹⁶ Most importantly, there have recently been successful reports^{20,21} of VCM for Cr_2O_3 films with resistivity values as low as $10^6 \Omega\text{cm}$. This places a useful lower constraint for the purpose of future device development.

While the discussion above makes clear the motivation for utilizing chromia in future spintronics, this field nonetheless remains at a nascent stage, with a strong need to optimize the electrical properties of this material. This is particularly true for the thin-film form of chromia, whose properties (as noted already) are already known to be strongly sensitive to the details of preparation. Motivated by this, we have undertaken a detailed electrical characterization of thin chromia films, deposited on various substrate materials (Pd, Pt and V_2O_3). These substrates were chosen due to their wide use in oxide-film synthesis, and exhibit different lattice mismatch (3.9% for Pd, 3.1% for Pt and 0.1% for V_2O_3 ²²) with chromia. Consequently, we are concerned with understanding the manner in which this influences the resulting dielectric properties of the chromia films. We find clear evidence for space-charge limited conduction (SCLC)^{23–25} in the films, and show that the details of this are sensitive to the choice of the underlying substrate. Most notably, the highest resistivity is obtained for chromia films fabricated on V_2O_3 substrates, consistent with the improved lattice matching to this material. We furthermore calculate various electrical properties for chromia, including its effective mobility, its total trap density, and its substrate-dependent trap distributions and energies. Based on these studies, we suggest that chromia thin films formed on V_2O_3 substrates are a promising candidate for next-generation ME spintronics.

II. ELECTRICAL CONDUCTION IN DIELECTRICS

To aid the analysis and understanding of our experimental results, in this section we give a brief overview of electrical-conduction mechanisms in thin dielectrics. SCLC is widely exhibited by such materials,^{23–25} and arises when current through the insulator becomes limited by the build-up of charge injected from the source electrode. This mechanism dominates once the applied voltage (V) reaches a characteristic value (V_{tr}), at which point the number of injected charge carriers in the vicinity of the source becomes equivalent to the number of thermally-generated ones.²⁶ At smaller voltages ($V < V_{tr}$), in contrast, thermal carriers provide the dominant contribution to the current, and ohmic conduction is consequently obtained. In the presence of these two mechanisms, the total current density may follow the functional form:

$$J = \alpha V + \beta V^2, \quad (1)$$

where the parameters α and β are associated with ohmic transport and SCLC, respectively. The defining equations for these parameters can be expressed as:^{27–30}

$$\alpha = \frac{nq\mu}{d} \quad (2)$$

$$\beta = \frac{9\mu\theta\epsilon_r\epsilon_0}{8d^3}. \quad (3)$$

In these expressions, n is the density of thermally generated charge carriers, q is the electronic charge, μ is the carrier mobility, d is the film thickness, ϵ_r is the dielectric constant and ϵ_0 is the permittivity of free space. θ is the ratio of free carriers to the total carrier concentration (i.e. free plus trapped charges). Assuming n -type material, this ratio can be expressed as:²⁶

$$\Theta = \frac{N_c}{g_n N_t} \exp\left(\frac{E_t - E_c}{k_B T}\right). \quad (4)$$

where g_n denotes the degeneracy of energy states in the conduction band, N_t is the total trap density, N_c is the effective density of states in the conduction band, E_t is the trap energy, E_c is the energy at the conduction band edge, k_B is the Boltzmann constant and T is the temperature. In samples free of traps, the parameter $\Theta = 1$. In the presence of traps, however, the value of Θ is voltage dependent, ultimately reaching unity once the last trap is filled.³¹ The product $\mu\Theta$ in Eq. (3) may be used to define an effective mobility, the value of which may be inferred directly from the observed current variations (as we demonstrate below).

Quite generally, the interplay of ohmic transport with SCLC leads to a four-stage conduction mechanism in dielectrics, as illustrated schematically in Fig. 1(a).^{26,31,32} Starting from the situation at

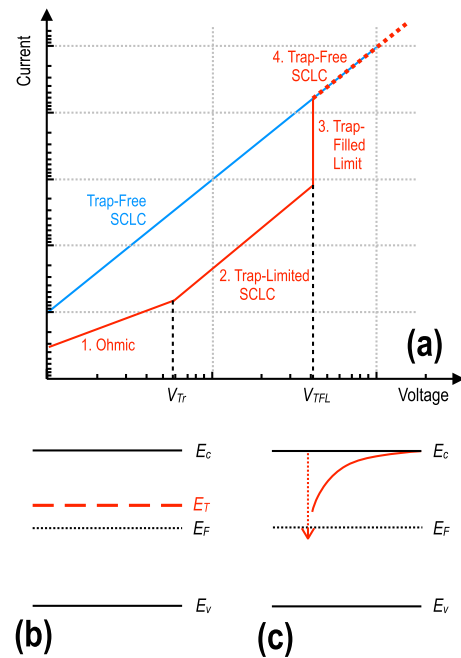


FIG. 1. (a) Schematic illustration of the typical form of the I - V characteristics exhibited by a dielectric in the presence of space-charge limited conduction (SCLC). (b) Discrete traps at a well-defined energy E_T . (c) Exponentially-distributed traps of the form of Eq. (6). The solid red line denotes the variation of $n_t(E)$, with the red dotted line corresponding to the energy axis (zero energy corresponds to the conduction-band edge, E_c).

low bias, these mechanisms are as follows: (1) ohmic-like conduction ($I \propto V^m$, $m = 1$); (2) trap-limited SCLC ($m = 2$); (3) the trap-filled limit (reached at voltage V_{TFL} , $m > 2$), and; (4) trap-free SCLC ($m = 2$). Dependent upon the nature of the defects in the material, a variety of I - V curves may therefore be exhibited. In an insulator free of traps, for example, only stages (1) and (4) will be observed. With discrete traps present (with energy E_T , see Fig. 1(b)), on the other hand, charge will begin to fill the traps at V_{tr} (see Fig. 1(a)), an estimate for which can be derived by equating both terms on the right side of Eq. (1) and determining the Θ term from Eq. (4). In this way it can be shown that the resulting value for V_{tr} can be expressed as:²⁶

$$V_{tr}(\text{discrete impurities}) = \frac{8qd^2g_nN_t}{9\epsilon_r\epsilon_0} \exp\left[-\frac{E_T - E_F}{k_B T}\right], \quad (5)$$

where E_F denotes the Fermi level. From this relation it is apparent that V_{tr} increases with increasing temperature. At voltages larger than this value, the second (β) term on the right-hand side of Eq. (1) dominates the current, as injected carriers overwhelm thermally-generated ones. However, once all traps are completely filled, implying that the quasi-static Fermi level is precisely aligned with the energy of the shallowest trap, a sudden increase in current (step 3 in Fig. 1(a)) will be observed.³¹ At even larger voltages than this, the I - V curve will once again resume its square-law dependence (step 4 in Fig. 1(a)), reflecting the influence of trap-free SCLC.

In some studies,^{33,34} it has been suggested that the traps in insulators should be distributed exponentially in energy (with a characteristic energy range E_t , see Fig. 1(c)). Under such an assumption, the trap distribution is expressed as:

$$n_t(E) = \frac{N_t}{k_B T} \exp\left(-\frac{E}{k_B T_c}\right), \quad (6)$$

where T_c is a temperature scale that defines the characteristic energy ($E_t = k_B T_c$) of the traps and E is the energy measured from the bottom of conduction band (again, assuming an n -type semiconductor). In this situation, the transition to the third stage of SCLC in Fig. 1(a) will no longer be sharply defined and the current will rather follow the expression:

$$J = q^{1-l} \mu N_c \left(\frac{2l+1}{l+1}\right)^{l+1} \left(\frac{l}{l+1} \frac{\epsilon_r \epsilon_0}{N_t}\right)^l \left(\frac{V^{l+1}}{d^{2l+1}}\right), \quad (7)$$

where $l = T_c/T$.

III. METHODS

Single-crystal chromia films (300-nm thick) were prepared on α - Al_2O_3 (0001) substrates, after first depositing a conductive layer to serve as a bottom electrode in electrical measurements. Our main focus here was on understanding the influence of this electrode material on the resulting dielectric properties of the films, to which end platinum, palladium, and vanadium oxide (V_2O_3) were utilized. Pt and Pd were selected since they are commonly used metals in semiconductor microfabrication, while V_2O_3 was utilized since it is a conductive oxide and so expected to be compatible, in many ways, with chromia. In a recent study where we explored the morphology of chromia synthesized on these films,²² we used conductive AFM to

show that electrical leakage was significantly reduced for chromia on V_2O_3 , a result that was attributed to the absence of twinning defects in that system. That having been said, no analysis was made of the leakage mechanisms in these films and it is this issue that forms the focus of this study.

The various conductive layers used to seed the chromia growth were synthesized via different methods, dictated by the specific properties of these crystalline layers. Molecular beam epitaxy (MBE) was used for the growth of a Pd(111), while Pt(111) films were deposited by DC magnetron sputtering, and V_2O_3 (0001) was grown by pulsed laser deposition (PLD). Typical thickness of these layers was around 25 nm.²² Following the growth of the bottom electrode, the samples were transferred to a PLD system and held at 700 °C. Chromia was then ablated from a (99.99% pure) ceramic target to deposit a thickness of 300 nm on the samples. X-ray diffraction analysis confirmed the good (0001) texture achieved for the chromia with different back electrodes. Twinning (i.e. 60° rotated domains) was observed in the Pd- and Pt-based crystalline films,²² consistent with previous observations.³⁵ (For further details on the synthesis and structural characterization of such films we refer the reader to Refs. 22, 35–38.)

Following thin-film growth, Cr(50nm)/Au(150nm) electrodes of area $50 \times 50 \mu\text{m}^2$ were fabricated on top of the chromia via a standard, photolithography and lift-off. Metal deposition was performed by electron-beam deposition, under a vacuum of less than 5 μTorr . I - V measurements of the films were then made with the samples mounted on the cold finger of a closed-cycle cryostat, under vacuum conditions below 1 μTorr and over the temperature range of 200 – 400 K. The latter range was chosen since V_2O_3 undergoes a metal-insulator transition near 160 K,^{39,40} below which this layer is unable to function as an efficient electrode.

IV. RESULTS

In our previous analysis of the electrical conductivity of chromia, grown on different metallic substrates, we found a significant statistical spread in the resistivity values, exhibited in measurements of nominally identical electrodes.²² In the study here, we focus on a comparison of the conductivity mechanisms exhibited by the most resistive of these contacts, since these are considered to be most indicative of the “intrinsic” nature of these materials. In Figs. 2(a)–2(c) we display representative I - V curves for the different chromia films. The main panels plot this data on linear axes, while in the lower insets the current is indicated on a logarithmic scale. Data are provided for the temperature range of 200 – 400 K and the overall behavior is qualitatively reminiscent of that observed for (bulk) chromia crystals.¹² The I - V curves exhibit pronounced nonlinearity, and the current increases strongly with increasing temperature, both indicators of the insulating nature of this material. In the upper inset to Fig. 2(c), we show the corresponding change of resistivity (calculated for an electric field of 33 kV/cm) of these films, as a function of temperature. From a comparison of these data we see that chromia exhibits its highest resistivity ($\sim 5 \text{ T}\Omega\text{cm}$ at 300 K) when synthesized on V_2O_3 , for which substrate the resistivity is close to that of crystalline chromia ($\sim 10 \text{ T}\Omega\text{cm}$ at 300 K).¹² The highest leakage, on the other hand, is found for chromia on Pd, for which the corresponding resistivity ($\sim 50 \text{ M}\Omega\text{cm}$ at 300 K) is almost six orders of magnitude smaller than that of chromia on V_2O_3 .

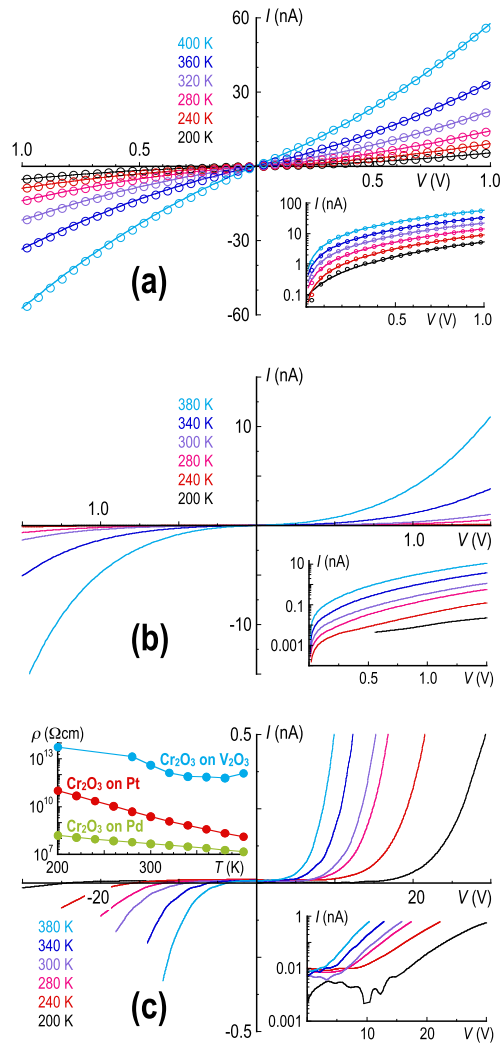


FIG. 2. (a) The main panel plots the temperature-dependent I - V characteristics of epitaxial chromia grown on Pd. Open circles are experimental data points (only 10% of which are shown) and solid lines are fits to the form of Eq. (1). The inset shows the same data, with current plotted on a logarithmic scale. (b) The main panel plots the temperature-dependent I - V characteristics of epitaxial chromia grown on Pt. The inset shows the same data, with current plotted on a logarithmic scale. (c) The main panel plots the temperature-dependent I - V characteristics of epitaxial chromia grown on V_2O_3 . The upper-left inset shows the temperature dependent resistivity of chromia on Pd, Pt and V_2O_3 , calculated at an electric field of 33 kV/cm. The lower-right inset shows the data of the main panel, with current plotted on a logarithmic scale.

Turning to a more detailed analysis of the current variations exhibited by the different films, for Cr_2O_3 on Pd we find that the I - V curves are well described by the form of Eq. (1). To illustrate this, in Fig. 2(a) we have used this relation to perform a two-parameter (α & β) fit to the measured currents. The fits are indicated by the solid lines and closely follow the experimental data, which are plotted using the open circles (for clarity, only 10% of data points are shown). The β term enables an estimate of the effective mobility

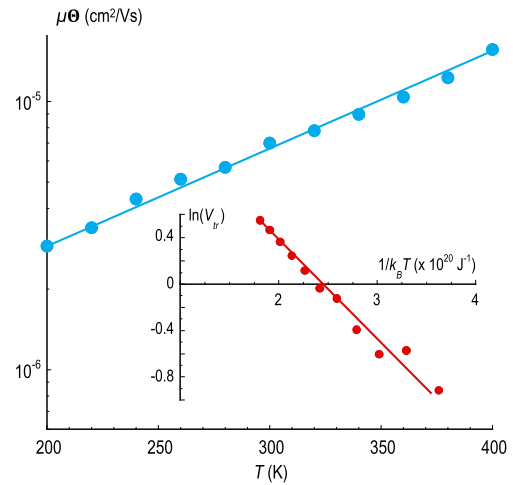


FIG. 3. The main panel plots the temperature-dependent variation of the effective mobility ($\mu\Theta$, see Eq. (3)), for the Pd-based chromia system. The inset plots the transition voltage (V_{tr}) as a function of temperature for the same film.

($\mu\Theta$, see Eq. (3)), and in the main panel of Fig. 3 we plot the variation of this quantity as a function of temperature. Much like the behavior reported for bulk chromia, and for numerous other insulators (See Ref. 12 and references therein), we find that this mobility increases exponentially with increasing temperature. Another parameter that may be inferred from the fits is the voltage (V_{tr}) at which SCLC exceeds ohmic conduction (defined as $V_{tr} = \alpha/\beta$, see Eq. (1)). For these particular films, V_{tr} increases with increasing temperature, a result that is consistent with the prediction of Eq. (5) for SCLC in the presence of discrete traps. To establish this connection explicitly, in the inset to Fig. 3 we plot $\ln(V_{tr})$ vs. $1/k_B T$ and find that the resulting data fall on a straight line. The slope of this line yields information on the trap energy E_T , and from the data in the figure we obtain $E_T - E_F \sim 50$ meV. While the value of the Fermi level in this material is not known *a priori*, its insulating character would tend to suggest a position somewhat close to midgap. Consequently, the inferred value of E_T points to the presence of deep traps, located well away from the conduction band. This conclusion can be reconciled with the results of a recent structural study,²² which has demonstrated a preponderance of twinning defects in chromia when it is grown on Pd. Calculations,⁴¹ based on density functional theory, suggest that these defects may give rise to a local reduction of the bandgap (by as much as 65%), in those regions corresponding to the boundary between neighboring, twinned domains. Such a reduction could be considered to be consistent with the presence of deep traps.

To understand the nature of the current variations exhibited by the other two types of film, in Fig. 4 we replot their I - V curves on double-logarithmic scales. In each of these panels, we observe a transition from ohmic conduction ($I \propto V^m$, $m \approx 1$) to SCLC ($m \geq 2$), as the magnitude of the applied voltage is increased. In contrast to the behavior exhibited by Cr_2O_3 on Pd, the voltage scale (V_{TFL}) associated with this transition is found to shift to smaller values with increasing temperature. Such behavior is consistent with expectations for materials whose traps are distributed exponentially within the gap (see Fig. 1(c) & Eq. (6)). Behavior of this kind has

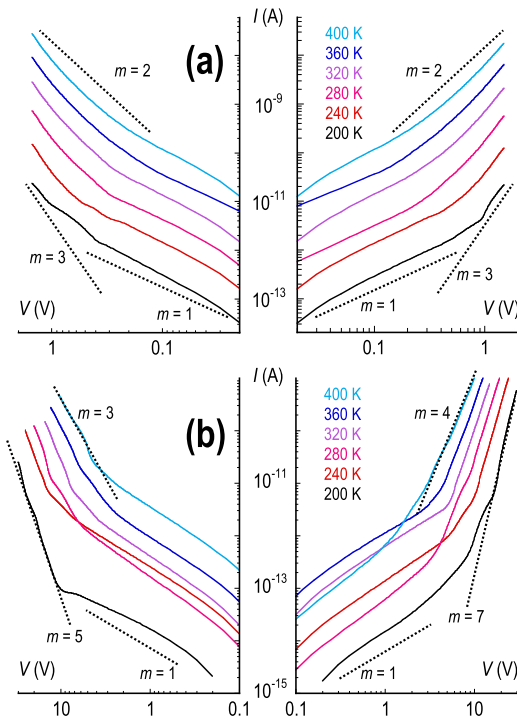


FIG. 4. The I - V curves for (a) chromia on Pt and (b) chromia on V_2O_3 , plotted on double-log scales to reveal the connection to Fig. 1(a). The different dotted lines are included as guides to the eye and denote different power-law variations of current (with index m) as a function of voltage. Left/right panels in both figures are for positive/negative voltage.

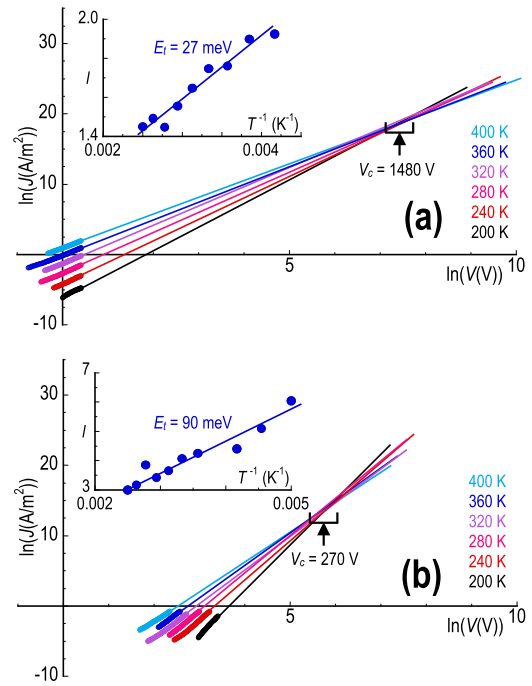


FIG. 5. (a) The main panel plots the SCLC component of the current (filled symbols) as a function of voltage, including its extrapolation to larger voltages (solid lines), for chromia on Pt. The Inset plots $I = (m + 1)$ as a function of inverse temperature in the same film. (b) The main panel plots the SCLC component of the current (filled symbols) as a function of voltage, including its extrapolation to larger voltages (solid lines), for chromia on V_2O_3 . The Inset plots I as a function of inverse temperature in the same film.

been reported previously for numerous dielectric materials,^{42–45} and is especially clear in the V_2O_3 -based films (Fig. 4(b)), in which the power-law exponent ($m = l + 1$) associated with SCLC increases from around 3 to 7 as the temperature is lowered over the indicated range.

In the insets Figs. 5(a) and 5(b), we plot the variation of the power-law index (l) as a function of $1/T$. The resulting data fall on a reasonable straight line, consistent with the definition of l in Eq. (7). The slope of the resulting straight line allows an estimate of the characteristic range (E_t) of the exponential trap distribution, and from the insets in Fig. 5 we infer $E_t = 27$ - & 90-meV for Cr_2O_3 on Pt and on V_2O_3 , respectively. In contrast to the case of the Pd-based films, these values correspond to trap distributions that are relatively shallow, lying close to the conduction band.

With an exponential distribution of traps, it is possible to make an estimate of the total trap density (N_t), by extrapolating the space-charge limited component of the current back to larger voltages. As we demonstrate in the main panels of Fig. 5, this yields a temperature-independent fixed point (V_c) at which the various I - V curves intersect one another. To obtain an analytical solution of V_c , we follow the treatment in Ref. 47 by writing Eq. (7) in an Arrhenius form to isolate the temperature dependence of the current. After some algebraic calculations, Eq. (7) may then be expressed as:⁴⁶

$$J = \left(\frac{\mu N_c q V}{d} \right) f(l) \exp \left[- \frac{E_t}{k_B T} \ln \left(\frac{q N_t d^2}{2 \epsilon_r \epsilon_0 V} \right) \right], \quad (8)$$

where:

$$f(l) = \left(\frac{2l + 1}{l + 1} \right)^{l+1} \left(\frac{l}{l + 1} \right)^l \frac{1}{2l}. \quad (9)$$

At the voltage V_c , the space-charge limited current is temperature independent and the form of Eq. (8) implies that:

$$V_c = \frac{q N_t d^2}{2 \epsilon_r \epsilon_0}. \quad (10)$$

By making use of Eq. (10), and the experimentally determined values of V_c from Fig. 5, we obtain the total trap densities $N_t = 2.1 \times 10^{19} \text{ cm}^{-3}$ & $3.2 \times 10^{18} \text{ cm}^{-3}$ for Cr_2O_3 on Pt and on V_2O_3 , respectively. These values fall within the range expected of high-quality insulating thin films.^{25,46,47} Interestingly, we note that the trap density is an order of magnitude smaller for Cr_2O_3 on V_2O_3 , which might be related to the improved lattice matching (with just 0.1% mismatch) in this system.

V. DISCUSSION

In this report, we have demonstrated how it is possible to use temperature-dependent measurements of current leakage in epitaxial chromia films, grown on different conducting substrates, and to infer quantitative information on the microscopic characteristics of their defects. The studies here suggest a fundamental

difference between chromia films grown on Pd, and those formed on Pt and V_2O_3 substrates, with the former being dominated by deep, discrete traps while the latter are characterized by the presence of exponentially-distributed, fairly shallow traps. This difference is consistent with what we have learned previously,²² from structural investigations of these films. These have shown that growth on Pd results in films with a preponderance of twinning defects, which function as highly-effective leakage paths. Theoretically, the leakage has been attributed to a 65% reduction of the chromia bandgap, which arises at the boundaries between neighboring twinning domains.⁴¹ At the same time, our analysis has shown that the leakage in these particular films may be attributed to the presence of deep traps, a result that could be consistent with such bandgap narrowing at localized positions. Our earlier work²² showed that the twinning defects can be suppressed through the growth of chromia on either Pt or V_2O_3 , consistent with which the microscopic nature of the defects in these films is found to be very different to that in Cr_2O_3 on Pd. The resulting traps are much shallower in energy, and distributed exponentially within the forbidden gap, in contrast to the discrete, deep traps inferred for Cr_2O_3 on Pd. The presence of such different trap distributions should, perhaps, not be altogether surprising; while the twinning defects are suppressed by growing chromia on either Pt or V_2O_3 , these materials are nonetheless known to exhibit dislocations that may function as an alternative source of trap(s).⁴⁸⁻⁵¹

VI. CONCLUSIONS

In conclusion, we have measured the temperature dependent (200 – 400 K) dielectric breakdown of high-quality, epitaxial chromia films, synthesized on various conductive substrates (Pd, Pt and V_2O_3). While we find evidence of SCLC in all of these materials, Pd-based chromia is found to exhibit behavior consistent with the presence of deep, discrete traps. The Pt- and V_2O_3 -based films, in contrast, show behavior typical of insulators with shallow, exponentially-distributed traps. The total trap density is approximately an order of magnitude smaller in the V_2O_3 -based films, a characteristic that appears consistent with the fact that the resistivity in this film system approaches that of bulk chromia. Overall, our results suggest that V_2O_3 -based Cr_2O_3 is a promising candidate for the implementation of next-generation spintronic devices.

ACKNOWLEDGMENTS

This work was supported in part by Antiferromagnetic Magneto-electric Memory and Logic (AMML), one of the centers in nCORE as task 2760.001, a Semiconductor Research Corporation (SRC) program sponsored by the NSF through ECCS 1740136. It was also supported by the Center for Nanoferroic Devices (CNFD), an SRC-NRI Nanoelectronics Research Initiative Center under Task ID 2398.001.

REFERENCES

- I. E. Dzyaloshinskii, *Sov. Phys. JETP* **10**, 628 (1960).
- T. J. Martin and A. C. Andersen, *IEEE Trans. Magnet. MAG-2*, 446 (1966).
- X. He, Y. Wang, N. Wu, A. N. Caruso, E. Vescovo, K. D. Belashchenko, P. A. Dowben, and C. Binek, *Nat. Mater.* **9**, 579 (2010).
- K. D. Belashchenko, *Phys. Rev. Lett.* **105**, 147204 (2010).
- N. Wu, X. He, A. L. Wysocki, U. Lanke, T. Komesu, K. D. Belashchenko, Ch. Binek, and P. A. Dowben, *Phys. Rev. Lett.* **106**, 087202 (2011).
- P. Borisov, A. Hochstrat, X. Chen, W. Kleemann, and C. Binek, *Phys. Rev. Lett.* **94**, 117203 (2005).
- N. Sharma, J. P. Bird, P. A. Dowben, and A. Marshall, *Semicond. Sci. Technol.* **31**, 065022 (2016).
- A. Iyama and T. Kimura, *Phys. Rev. B* **87**, 180408(R) (2013).
- E. W. A. Young, P. C. M. Stiphout, and J. H. W. de Wit, *J. Electrochem. Soc.* **132**, 884 (1985).
- K. P. Lillerud and P. Kofstad, *J. Electrochem. Soc.* **127**, 2397 (1980).
- R. Cheng, B. Xu, C. N. Borca, A. Sokolov, C.-S. Yang, L. Yuan, S.-H. Liou, B. Doudin, and P. A. Dowben, *Appl. Phys. Lett.* **79**, 3122 (2001).
- C.-P. Kwan, R. Chen, U. Singiseti, and J. P. Bird, *Appl. Phys. Lett.* **106**, 112901 (2015).
- E. W. A. Young, P. C. M. Stiphout, and J. H. W. de Wit, *J. Electrochem. Soc.* **132**, 884 (1985).
- R. C. Ku and W. L. Winterbottom, *Thin Sol. Films* **127**, 241 (1985).
- C.-S. Cheng, H. Gomi, and H. Sakata, *Phys. Status Solidi A* **155**, 417 (1996).
- S.-H. Lim, M. Murakami, S. E. Lofland, A. J. Zambano, L. G. Salamancha, and I. Takeuchi, *J. Magn. Magn. Mater.* **321**, 1955 (2009).
- M. D. Julkarnain, J. Hossain, K. S. Sharif, and K. A. Khan, *J. Optoelectron. Adv. Mater.* **13**, 485 (2011).
- S.-C. Chen, T.-C. Chang, S.-Y. Chen, H.-W. Li, Y.-T. Tsai, C.-W. Chen, S. M. Sze, F.-S. Yeh (Huang), and Y.-H. Tai, *Electrochem. Solid-State Lett.* **14**, H103 (2011).
- M. M. Abdullah, F. M. Rajab, and S. M. Al-Abbas, *AIP Adv.* **4**, 027121 (2014).
- K. Toyoki, Y. Shiratsuchi, A. Kobane, C. Mitsumata, Y. Kotani, T. Nakamura, and R. Nakatani, *Appl. Phys. Lett.* **106**, 162404 (2015).
- T. Ashida, M. Oida, N. Shimomura, T. Nozaki, T. Shibata, and M. Sahashi, *Appl. Phys. Lett.* **106**, 132407 (2015).
- A. Mahmood, M. Street, W. Echtenkamp, C. P. Kwan, J. P. Bird, and C. Binek, *Phys. Rev. Mater.* **2**, 044401 (2018).
- S. T. Chang and J. Y.-M. Lee, *Appl. Phys. Lett.* **80**, 655 (2002).
- S. Farokhipoor and B. Noheda, *Phys. Rev. Lett.* **107**, 127601 (2011).
- P. E. Burrows, Z. Shen, V. Bulovic, D. M. McCarty, S. R. Forrest, J. A. Cronin, and M. E. Thompson, *J. Appl. Phys.* **79**, 7991 (1996).
- F. C. Chiu, *Adv. Mater. Sci. Eng.* **2014**, 578168.
- M. A. Lambert and P. Mark, *Current Injection in Solids* (Academic Press, New York, NY, USA, 1970).
- N. F. Mott and E. A. Davis, *Electronic Processes in Non-Crystalline Materials* (Oxford University Press, Oxford, UK, 1979).
- K. C. Kao, *Dielectric Phenomena in Solids* (Academic Press, New York, NY, USA, 2004).
- J. F. Scott, *J. Phys.: Condens. Matt.* **26**, 142202 (2014).
- G. G. Raju, *Dielectric in Electric Fields* (CRC Press, Taylor & Francis Group, 2017), Ch. 10.
- M. A. Lampert, *Phys. Rev.* **103**, 1648 (1956).
- D. S. Shang, Q. Wang, L. D. Chen, R. Dong, X. M. Li, and W. Q. Zhang, *Phys. Rev. B* **73**, 245427 (2006).
- T. H. Chiang and J. F. Wager, *IEEE Trans. Electron Dev.* **65**, 223 (2018).
- T. Wagner, G. Richter, and M. Ruhle, *J. Appl. Phys.* **89**, 5 (2001).
- M. Street, W. Echtenkamp, T. Komesu, S. Cao, P. A. Dowben, and Ch. Binek, *Appl. Phys. Lett.* **104**, 222402 (2014).
- J. Brockman, M. G. Samant, K. P. Roche, and S. S. P. Parkin, *Appl. Phys. Lett.* **101**, 051606 (2012).
- B. S. Allimi, S. P. Alpay, C. K. Xie, B. O. Wells, J. I. Budnick, and D. M. Pease, *Appl. Phys. Lett.* **92**, 202105 (2008).
- M. Imada, A. Fujimori, and Y. Tokura, *Rev. Mod. Phys.* **70**, 1039 (1998).
- G. Keller, K. Held, V. Eyert, D. Vollhardt, and V. I. Anisimov, *Phys. Rev. B* **70**, 205116 (2004).
- C. Sun, Z. Song, A. Rath, M. Street, W. Echtenkamp, J. Feng, C. Binek, D. Morgan, and P. Voyles, *Adv. Mater. Interf.* **4**, 1700172 (2017).

- ⁴²P. Mark, *J. Appl. Phys.* **33**, 205 (1962).
- ⁴³F. C. Chiu, *J. Appl. Phys.* **102**, 044116 (2007).
- ⁴⁴M. J. Speirs, D. N. Dirin, M. Abdu-Aguye, D. M. Balazs, M. V. Kovalenko, and M. A. Loi, *Energy Environ. Sci.* **9**, 2916 (2016).
- ⁴⁵F. C. Chiu, H. W. Chiu, and J. Y.-M. Lee, *J. Appl. Phys.* **97**, 103503 (2005).
- ⁴⁶V. Kumar, S. C. Jain, A. K. Kapoor, J. Poortmans, and R. Mertens, *J. Appl. Phys.* **94**, 1283 (2003).
- ⁴⁷S. Berleb, A. G. Muckl, W. Brutting, and M. Schwoerer, *Synth. Met.* **111-112**, 341 (2000).
- ⁴⁸C. Sun, Structure study of magnetic thin films for voltage controlled spintronics by scanning transmission electron microscope experiment and density functional theory calculations, Ph.D thesis, University of Wisconsin-Madison (2018).
- ⁴⁹J. F. Shackelford, *Introduction to Materials Science for Engineers* (Pearson, 2015).
- ⁵⁰T. Wosinski, *J. Appl. Phys.* **65**, 1566 (1998).
- ⁵¹J. E. Dominguez, L. Fu, and X. Q. Pan, *Appl. Phys. Lett.* **81**, 5168 (2002).